

# UNCERTAINTY PROPAGATION THROUGH THERMO-HYDRO-MECHANICAL MODELLING OF CONCRETE CRACKING AND LEAKAGE – APPLICATION TO CONTAINMENT BUILDINGS

J. BAROTH<sup>\*</sup>, D. E.-M. BOUHJITI<sup>\*,†</sup>, F. DUFOUR<sup>\*</sup> AND M. BRIFFAUT<sup>\*</sup>

<sup>\*</sup> Univ. Grenoble Alpes, CNRS, Grenoble INP<sup>1</sup>, 3SR, F-38000 Grenoble, France

<sup>†</sup> EGIS Industries, 4 rue Dolores Ibarruri Montreuil, TSA 50012-93188, France

e-mail: julien.baroth@3sr-grenoble.fr, www.3sr-grenoble.fr

**Key words:** concrete, large buildings, THM, Leakage, SFEM, uncertainty propagation, sensitivity analysis

**Abstract:** The prediction of the Thermo-Hydro-Mechanical (THM) behavior of large buildings with a containment role (reservoirs, dams, nuclear vessels, etc.) is a critical step towards their risk assessment. In particular, their cracking implies a considerable loss of their structural tightness that needs to be controlled, monitored and, if necessary, repaired to ensure a safe operational environment. The difficulty of performing numerical predictive analyses is related to (a) the multi-phasic and multi-physical nature of concrete (b) the large number of inputs to identify at the specimen and structural scales (c) the non-negligible and intrinsic material and load related uncertainties. All these aspects strongly affect our ability to foresee the structural response of large constructions; especially in terms of cracking and tightness. In this contribution, a global finite elements based stochastic methodology is proposed to allow physically representative and efficient non-intrusive probabilistic coupling of strongly nonlinear and numerically expensive THM calculations. To this aim (a) concrete cracking is modeled using a stochastic, local and energy regularized damage model accounting for size effects (b) concrete permeability is defined using a strain-based law (c) the spatial heterogeneity of properties is modeled using discretized and FE projected Random Fields (d) uncertainties propagation is computed using adapted Surface Response based methods. For the demonstration of this strategy's efficiency and effectiveness, in terms of physical accuracy and cost optimization, a 1:3 scaled containment building named VeRCoRs is considered as an application. In particular, a complete probabilistic analysis of its dry air leakage rate (indicative of the whole structural performance) is achieved within a computational time of tens of days only. In general, such results can help during the decision-making process for the design, maintenance and risk assessment of large structures with a containment role based on a leakage-rate-defined criterion under service loads.

---

<sup>1</sup> Institute of Engineering Univ. Grenoble Alpes

## 1 INTRODUCTION

The durability of strategic and large concrete structures is strongly affected by the aging of the concrete material and the time evolution of its properties under variable and simultaneous Thermo-Hydro-Mechanical (THM) loads. In particular, for buildings with a containment role (reservoirs, dams, nuclear vessels, etc.), their structural and functional performances under service loads are dependent mainly on their damage state which reduces their structural rigidity and tightness. Though several models exist to deal with such topic, the numerical blind prediction of their behavior remains a complex task; especially when considering the:

- Intrinsic spatial variability of concrete properties and their time evolution.
- Inherent spatiotemporal variability of the applied service THM loads
- Limited computational resources at our disposal which do not allow the use of classical Monte Carlo Methods (MCM) to analyze uncertainties propagation through the used model and perform a full probabilistic analysis of the possible damage scenarios and their consequences.

Accordingly, the reduction of the epistemic error in our models is dependent on the constant improvement of our physical knowledge, but mostly on the introduction of uncertainties in our calculations within a probabilistic framework instead of a classical deterministic one using adapted and time-efficient mathematical methods.

In particular, the simulation of concrete cracking in large structures is still mainly performed in a deterministic way [1-2] though it strongly depends on the way concrete's mechanical properties are scattered (especially the tensile strength [3] and the Young's modulus [4]). On one hand, and to address such limitation, several authors have chosen to explicitly model concrete's spatial heterogeneities using discretized and FE-

projected Random Fields [5-6]. Nevertheless, such choice implies the use of MCM to achieve a proper statistical analysis which becomes quickly unreasonable given the hefty computational time of damage models under THM loads; especially at the structural scale (estimated at hours and days [1][7]). Accordingly, a more efficient stochastic analysis method is required for the modeling of concrete cracking.

On the other hand, sources of concrete damage might be of other nature than the mechanical one; for instance of chemical, thermal or hydric nature [1][2][7]. Therefore, uncertainties should not be limited to the mechanical properties and loads but need to be extended to all phenomena affecting concrete behavior from its early ages [8] throughout its operational lifespan [9]. This implies the consideration of a large number of parameters (thermo-hydration, drying, creep, etc.). In that sense, one can find in the literature several sensitivity or stochastic analysis limited to one calculation step (T or H or M or their effects on the Leakage rate L) or a single time period (early age or long term) using simplified models (analytical, 0D, 1D, 2D approaches) [10-12]. Though such efforts are worth exploring for engineering purposes, a full THM-L calculation strategy under uncertainties is still lacked for a more inclusive performance and risk assessment for large structures; especially given the non-negligible uncertainty amplification through the THM-L behavior.

Accordingly, this contribution aims at the enhancement of the physical accuracy and the risk control of concrete THM-L behavior under material and load related intrinsic uncertainties using convenient stochastic methods:

- The first part presents a weakly coupled THM-L model and recalls its main hypotheses and improvements compared to existing ones.

- The second part details the global stochastic approach in the case of THM-L analysis in a two-step process aiming at the identification of most influential inputs before achieving uncertainties propagation.
- The third and last part is an application of the stochastic THM-L model to the case of an experimental 1:3 containment building. Through the provided results, the physical validity and cost convenience of the presented strategy are demonstrated.

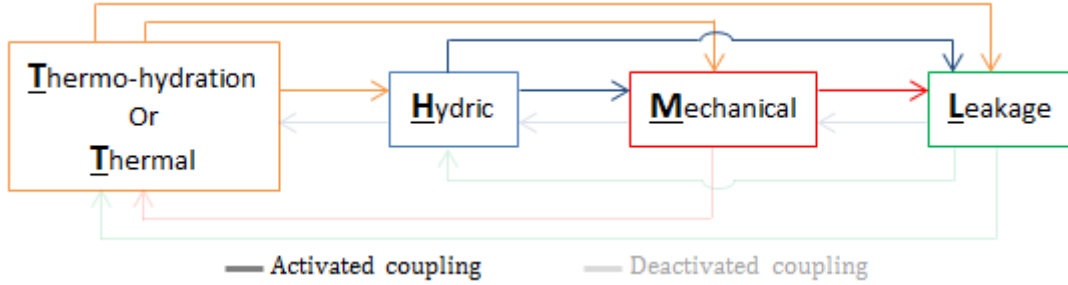


Figure 1: Weakly staggered THM+L model for the modeling of large concrete buildings' behavior.

## 2.1 Thermal calculations

The first calculation step corresponds to the solving of the heat equation in its general form; including a non-null source term for the hydration process simulation:

$$\rho_c C_c^p \frac{dT}{dt} - \lambda_c \nabla^2 T = Q_{th} \quad (1)$$

where  $\rho_c$  is the concrete's mass density,  $C_c^p$  the thermal capacity,  $\lambda_c$  is the thermal conductivity,  $Q_{th}$  the hydration heat that tends to zero as the hydration rate tends to 1.

## 1.2 Hydric calculations

The second calculation phase requires solving the heat equation where the water content  $C_w$  is the main unknown. This is achieved through the use of a phenomenological and non-linear diffusivity factor  $D_w$ . The early age effect is accounted for by defining an initial water content from which the chemically bonded water (non-evaporable) is removed. So, the water loss by drying is decoupled from water consumption due to hydration.

$$\frac{dC_w}{dt} - \nabla \cdot (D_w \nabla C_w) = 0 \quad (2)$$

$$C_{w,0} = w - 0.23 c \quad D_w = A_w e^{B_w C_w} f(T)$$

where  $w, c$  are the water and cement content in the

## 2 THM-L MODEL

The considered model hereafter is based on a staggered THM-L framework (Fig. 1) that has been developed and validated in previous works [7][13-14] in the case of full and 1:3 scale containment buildings. This section provides the main hypotheses, descriptive equations and inputs of such model.

design mix respectively ( $\text{kg/m}^3$ ),  $A_w, B_w$  fitting parameters and  $f(T)$  a thermo-activation function.

## 1.3 Mechanical calculations

The third calculation phase consists of solving the mechanical problem within a damageable and viscoelastic framework. The total strain  $\epsilon_{TOT}$  is divided into five components:

$$\epsilon_{TOT} = \epsilon_{ELAS} + \epsilon_{TH} + \epsilon_{ES} + \epsilon_{DS} + \epsilon_{CR} \quad (3)$$

where  $\epsilon_{ELAS}$  is the elastic strain tensor,  $\epsilon_{TH}$  the thermal strain tensor related to the temperature variation in time,  $\epsilon_{ES}$  the endogenous shrinkage tensor related to the hydration rate,  $\epsilon_{DS}$  the drying shrinkage tensor related to the water content variation in time and  $\epsilon_{CR}$  the basic and drying creep tensor.

Relative humidity dependent basic and drying creeps are computed using the Burgers model [7] based on the water migration theory. The dependence on the hydration rate is defined according to the maturity method and thermo-activation is defined using the Arrhenius law. As for concrete damage modeling (eq. 4), a strain-based, unilateral, local and energy-regularized model accounting for the contribution of creep is used [15].

$$\boldsymbol{\sigma} = (1 - d)\mathbf{C}_0 : \boldsymbol{\varepsilon} \quad (4)$$

with  $d$  the scalar damage variable,  $\mathbf{C}_0$  the elastic stiffness tensor,  $(\boldsymbol{\sigma}, \boldsymbol{\varepsilon})$  the stress and strain tensors respectively.

Given the continuous formulation of damage, the crack openings are post-processed directly from the damage and strain fields [16]. Finally, size effects are taken into account in a two-step process [7]:

(a) By using a probabilistic based Size Effect Law (SEL) where the tensile strength is directly linked to the effective volume under tensile loads.

(b) By introducing explicitly in the FE model the spatial variability of concrete properties – namely the Young’s modulus – using Random Fields.

The combination of the two steps allows a size-dependent and spatially variable tensile behavior law of concrete in terms of the damage strain threshold and its softening behavior.

### 1.4 Leakage calculations

The fourth and last calculation step consists of post-processing the air permeability of concrete  $k_{eq}$  and solving the air transfer equation under imposed pressure gradient  $\Delta P_{air}$ .

$$P_{air}^{\cdot} = \nabla \cdot \left( \frac{k_{eq}}{2 \mu_{air}} \nabla \cdot P_{air}^2 \right) \quad (5)$$

where  $\mu_{air}$  is the dynamic viscosity of the air.

To define the concrete’s permeability, two transfer modes are considered [16]:

- The first for a microcracked mechanical state where the damage variable is low (less than 20%). The hypothesis of concrete as a homogeneous domain is then valid which leads to the acceptance of Darcy’s law as a governing air transfer mode. The associated permeability  $k_D$  writes, including the effects of permeability and slip flow (Klinkenberg effect):

$$k_D = k_0 \cdot f_1(S_r) \cdot f_2(P_{air}, S_r) \cdot (f_3^r(\varepsilon) + f_3^i(\varepsilon)) \quad (6)$$

where  $f_1$  a term to account for the saturation rate  $S_r$ ,  $f_2$  a term descriptive of the Klinkenberg effect,  $f_3^r$  and  $f_3^i$  two strain-dependent terms (the first reversible and the second irreversible) to account for the low damage state in concrete.

- The second for a macrocracked mechanical state where the strain localization induces a strong discontinuity within the concrete volume which can no longer be described using Darcy’s law; instead the Poiseuille’s law is used:

$$k_F = \xi \frac{w_{ck}^3}{12 h_{EF}} \quad (7)$$

where  $w_{ck}$  is the crack opening,  $h_{EF}$  the FE characteristic size and  $\xi$  a correcting factor to account for the cracks’ roughness and shape on the air transfer.

As one can notice, the two modes have different validity domains. To allow a continuous description of permeability with the mechanical state, a strain-weighted log-type matching law is used:

$$k_{eq} = (k_D)^{1-p} \cdot (k_F)^p \quad (8)$$

$$p = \left( \frac{< d_r - d_{lim} >_+}{1 - d_{lim}} \right)^\delta$$

where  $p$  is a strain-based weighting factor active when the low damage threshold of  $d_{lim} = 0.2$  is exceeded.

### 3 STOCHASTIC THM-L MODELING

The previous THM-L model involves a considerable number of parameters (more than 60) and strong non-linearities in the mathematical models inducing hefty computational time; especially at large scale. Therefore, to achieve the probabilistic analysis within a reasonable cost, a first step would be to define the most influential parameters and parameters before aiming at uncertainties propagation. This is supported by the fact that not all parameters or phenomena affect concrete cracking response in the same way and it would be reasonable to gear our interest towards the most influential ones only. Once, such inputs are defined, metamodeling techniques can be used to approach the FE response and provide an explicit THM-L model to which Monte Carlo Methods would

be easily applicable. Such strategy is depicted in Fig. 2 and, in details, consist of pursuing the following steps (where the first two have already been tackled in the introduction and section 2):

- 1<sup>st</sup> step – functional and structural analysis of the building of interest
- 2<sup>nd</sup> step: definition of an appropriate valid THM-L model
- 3<sup>rd</sup> step – uncertainties quantification of the model’s inputs
- 4<sup>th</sup> step – sensitivity analysis of

the model and identification of the most influential parameters

- 5<sup>th</sup> step – uncertainties propagation through the THM-L model by means of adapted Surface Response Methods to which Monte Carlo Method could be applied straightforwardly.
- 6<sup>th</sup> step – analysis of the structural performance based on the probabilistic and reliability analyses of the outputs of interest.

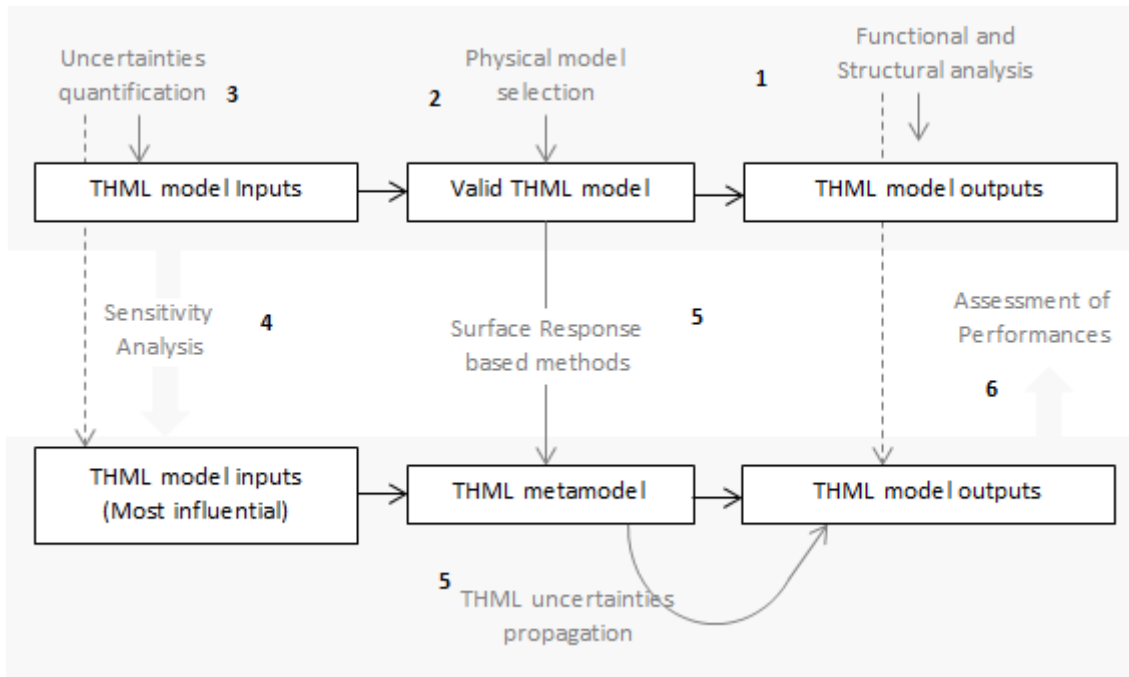


Figure 2: Global strategy for the stochastic THM-L analysis of large concrete structures [17].

### 3.1 Sensitivity analysis

Given the large number of inputs and the computational time of each THM-L calculation, our interest is geared towards Local Sensitivity Analyses (LSA) which are less costly compared to the Global ones (GSA)<sup>2</sup>. Indeed, our goal is to define the most influential parameters even qualitatively; though the approximation of the statistical

moments might be less precise. With that regard, the OFAT-based approach [18] (One-Factor-at-A-Time) is the best candidate. After defining the variation domains of each input of the N inputs  $x_i^- \leq x_{1 \leq i \leq N} \leq x_i^+$ , the OFAT method consists of running the model y for each one of its inputs  $x_i$  at its upper  $x_i^+$  and lower  $x_i^-$  bounds whilst the rest of inputs  $x_{j \neq i}$  is maintained at its mean value; in addition to a reference calculation where all inputs are at their mean values  $x_i^0$ . Eventually, the cost of such analysis is minimal of  $2 \cdot N + 1$  for a model y with N inputs. Then, one might estimate the partial variance  $(\sigma_i^y)^2$  of the output y to the

<sup>2</sup> The main drawback of local approaches is that their associated derivatives provide information only at the base point where they are computed; whereas the global ones take into account the rest of the variation range of the model’s parameters.

variation of the input  $x_i$ :

$$\begin{aligned} \mu_i^y &= y(x_i^0) = \mu^y \\ (\sigma_i^y)^2 &= \text{Var}[y(x_i^-); y(x_i^0); y(x_i^+)] \end{aligned} \quad (9)$$

A qualitative order can then be achieved based on the contribution of each input  $x_i$  to the total variance  $\sum_{i=1}^N (\sigma_i^y)^2$  proving an index:

$$I_i^y = \frac{(\sigma_i^y)^2}{\sum_{j=1}^N (\sigma_j^y)^2} \quad (10)$$

Those indicators, once classified, lead to a hierarchized list of parameters according to their influence on the model  $y$  (for instance, one can retain the first ones that contribute by more than 90% to the total variance).

Additionally, given the staggered scheme of the retained THM-L model; one can further gain time by performing an adaptive or hierarchized sensitivity analysis by retaining only the most influential parameters at a given calculation step to perform sensitivity analysis of the next one. For example, let's assume that only 2 thermal inputs are influential on the thermal response of concrete. Then, it is reasonable to say that only those two would be influential on the HM-L response in addition to the other HM-L parameters, and so forth. Eventually, the number of model calls is reduced as the number of potentially influential inputs is reduced at each step.

### 3.2 THM-L metamodeling

In this section, our interest is geared towards Spectral Methods which aim at fitting the model's FE response to a finite development using a limited number of model calls; in particular the Polynomial Chaos Expansion is of interest [19].

For each THM-L model response, and considering the most influential inputs only from the previous Hierarchized Local Sensitivity Analysis (HLSA), a truncated polynomial approximation can be derived:

$$y(x) \approx \hat{y}(x) = \sum_{\alpha=0}^{Q < +\infty} y_{\alpha} \Psi_{\alpha}(X) \quad (11)$$

where  $X$  the list of influential random and independent inputs,  $\{\Psi_{\alpha}\}$  an orthonormal polynomial basis in the associated Hilbertian space,  $\{y_{\alpha}\}$  the polynomial coefficients and  $Q$  the truncation order.

The truncating order  $Q$  is to be defined based on one or a combination of the following criteria: computational time limitation, relative error  $\frac{|y(x) - \hat{y}(x)|}{y(x)}$  or absolute error  $|y(x) - \hat{y}(x)|$ , a given variance or mean error norm  $\left| \left| \sigma_y^2 - \sigma_{\hat{y}}^2 \right| \right|$  or  $\left| \left| \mu_y - \mu_{\hat{y}} \right| \right|$ , etc. Once the metamodel is defined and its approximation of the real FE model validated, Crude Monte Carlo Method can be applied at low cost and so is a variance-based GSA.

## 4 APPLICATION TO NUCLEAR CONTAINMENT BUILDINGS

### 4.1 Overview of the VeRCoRs mock-up

The functional role of Nuclear Containment Buildings (NCB) consists of protecting the environment from radioactive substances under operational loads or in the unfortunate case of a nuclear accident. For double walled NCBs, the structural tightness is ensured by the inner wall made out of reinforced and prestressed concrete. For full scale NCBs, the regulatory threshold for the dry air leakage is set, by the French Nuclear Safety Agency, to 1.5% of the total gas mass inside the inner building per day under a pressure gradient of 4.2 bars. EDF proceeds to such verification in a periodic way (once every decade) and considers an additional safety margin to account for ageing of concrete between the required pressurization tests. This brings the threshold to a safer margin of 1.1%.

Due to aging phenomena, the structural air tightness of NCBs decreases over time. Amongst the main reasons there are:

- Cracking at early age induced by the heterogeneous structural rigidities of concrete lifts, thermal and endogenous restraining effects.

- Drying of concrete (especially for operational temperatures around 35°C) leads to a loss of water content and to the increase of the concrete's mass air permeability.
- Prestressing losses which are related to concrete creep and drying increasing the risk of early age cracks reopening under pressurization loads.
- Existence of local defects at the casting joints, etc. responsible for additional leakage rate – though marginal compared to the one through the concrete's mass and its cracks –.

In this application part, a 1:3 scaled NCB (Fig. 3) is considered for the stochastic analysis of the leakage rate (one of the main outputs of interest) in order to quantify the risk of exceeding the regulatory threshold based on the various intrinsic uncertainties of the THM-L model inputs (both material and load related ones).

For the sake of conciseness, intermediate THM results analyses are not shown (but can be found in [17]) and the main focus is granted to the final calculation step in terms of air leakage estimation.

#### 4.2 FE model

To reduce numerical cost and allow refined mesh for such large structure modeling, numerical calculations are performed at the scale of Representative Structural Volumes (RSV) shown in Fig. 3. The dimensions of each RSV are defined so as to ensure the objectiveness and representativeness of the applied boundary conditions, of the material spatial scattering and of the external loads spatial variability. Also, so as to reproduce as accurately the restraining effects and the structural ones, each RSV is modeled including a realistic representation of steel rebars, stirrups and prestressing sheaths and cables using 1D FE segments to which effective sections are associated.

In terms of boundary conditions, Neumann exchange modes are applied for thermal and hydric calculations based on realistic in situ

measurements of temperature and relative humidity. And for the mechanical boundary conditions, axisymmetric ones are applied on the lateral edges throughout the analysis and the upper surfaces of each RSV are supposed to have uniform vertical displacement (the tangential and vertical directions correspond to the principal ones for a cylindrical coordinate system associated to the NCB structure). One should note that the steel elements are only active during the mechanical calculations using a perfect steel-concrete bond. Tab. 1 sums up relevant inputs for the numerical study. The full list of inputs is available in [17].

**Table 1:** Distributions of the most influential THM-L inputs [17]

Parameter	Mean	CV (%)	Distribution
$Q_{\infty}(\text{MJ}/\text{m}^3)$	82	40	$\text{Log}^1$
$C^P(\text{J}/(\text{kg} \text{ } ^\circ\text{K}))$	0.88	40	$\text{Log}^1$
$B_w$	0.05	20	$\text{Log}^1$
$C_{w,0}(\text{litre}/\text{m}^3)$	132	20	$\text{Log}^1$
$E(\text{GPa})$	36	10	$\text{Log}^2$
$R_t(\text{MPa})$	4.5	10	$\text{Log}^2$
$\alpha_{ES}(\mu\text{m}/\text{m})$	70	10	$\text{Log}^1$
$\alpha_{TH}(\mu\text{m}/(\text{m} \text{ } ^\circ\text{K}))$	10	10	$\text{Log}^1$
$\alpha_{DS} \left( \frac{\mu\text{m}}{\text{m}} / \frac{\text{litre}}{\text{m}^3} \right)$	7.1	10	$\text{Log}^1$
GUSSET $\sigma_{PRES}^T(\text{MPa})$	0.8	50	$\text{Log}^3$
$\sigma_{PREC}^T(\text{MPa})$	0.5	50	$\text{Log}^3$
$k_0(\text{m}^2)$	$2.7 \cdot 10^{-17}$	50	$\text{Log}^3$

<sup>1</sup> Experts' judgment – principle of maximum entropy

<sup>2</sup> Experimental data at the specimen scale

<sup>3</sup> Experimental data at the structural scale

As for the air leakage rate estimation, the superposition principle is applied considering that the structural air leakage rate is the sum of all its RSVs':

$$Q_{\text{total}} = Q_{\text{GUSSET}} + Q_{\text{WALL}} + Q_{\text{EAH}} + Q_{\text{DOME}}$$

$$\begin{cases} Q_{\text{GUSSET}} = 24 * Q_{\text{GUSSET}}^{\text{RSV}} \\ Q_{\text{WALL}} = 268 * Q_{\text{WALL}}^{\text{RSV}} \\ Q_{\text{EAH}} = 4 * Q_{\text{EAH}}^{\text{RSV}} \\ Q_{\text{DOME}} = 24 * Q_{\text{DOME}}^{\text{RSV}} \end{cases} \quad (12)$$

#### 4.3 HLSA results

Throughout the THM-L sensitivity analysis,

the number of influential inputs has been reduced by more than 80%. Only 9 of them contribute to more than 90% of the total variance of the total air leakage rate through

the VeRCoRs' structure  $Q_{total}$  (Fig. 4). Those parameters and their corresponding phenomena are as following (Tab. 1 and 2):

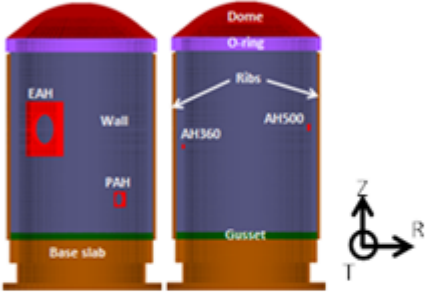
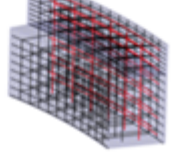
Full	Structural Volumes	Representative Structural Volumes
$h_{EF} = 30 - 60 \text{ cm}$		$h_{EF} = 1 - 8 \text{ cm}$
 <p>NE: 196 280</p> <p>NE=Number of finite Elements</p>	Dome + O-ring	
	4 lifts - 360°	4 lifts - 15°
		
	NE: 53874	NE: 32205
	EAH	
	6 lifts - 60°	3 lifts - 30°
		
NE: 1940	NE: 8596	
Wall		
12 lifts - 360°	1 lift - 15°	
		
NE: 67090	NE: 4256	
Gusset + Base slab		
2 lifts - 360°	1 lift - 15°	
		
NE: 73000	NE: 3456	

Figure 3: VeRCoRs mock-up FE model and RSV-based decomposition for full scale analysis within a probabilistic framework.

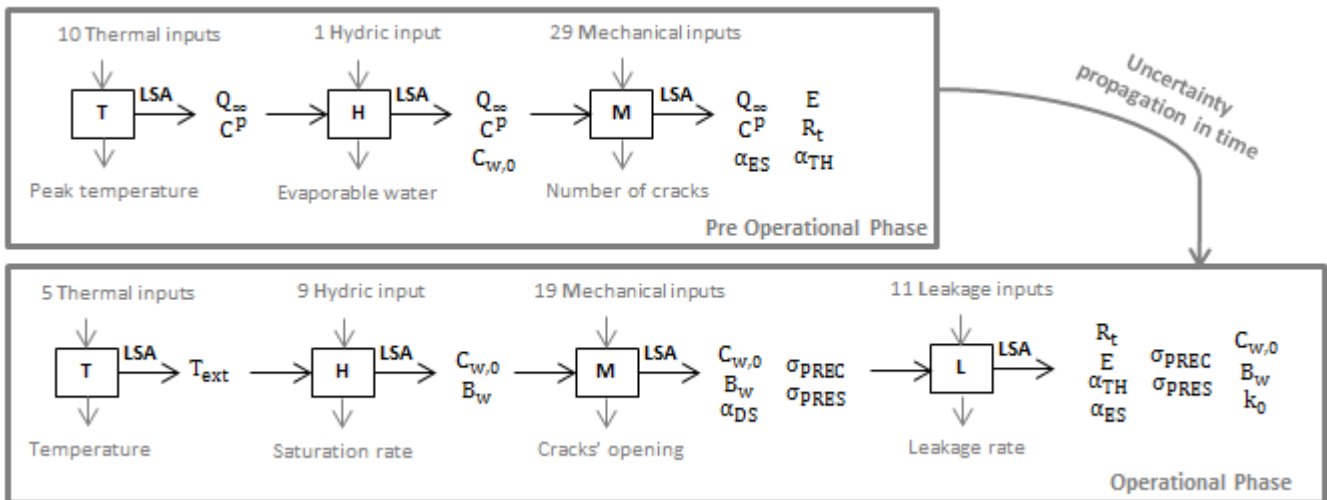


Figure 4: Application of the HLSA method to the THM-L behavior of concrete for the identification of the most influential parameters per T, H, M, L calculation step and per time phase (pre operational and operational).

- Early age cracking phenomena: Five inputs (two thermal:  $Q_{\infty}, C^P$  and three mechanical:  $E, R_t, \alpha_{TH}, \alpha_{ES}$ ) seem to affect concrete cracking at early age; namely the number of cracks per gusset's RSV (for other RSVs the risk of cracking remains low). The thermal ones are linked to the thermo-hydration phase and are directly responsible for the variance of the peak temperature at early age which defines the amplitude of the thermal shrinkage during the cooling phase. As for the mechanical ones, they refer to size effects mainly as they define the strain damage threshold and also the amount of the thermal and chemically restrained shrinkages.

- Drying phenomena: two hydric inputs considerably affect the drying process of concrete. One ( $B_w$ ) is related to the diffusivity factor defined by the porous network connectivity and the other ( $C_{w,0}$ ) related to the concrete mix and evaporable water after the hydration phase. Their effect is not limited on the air permeability of the mass but concerns, in addition to the drying shrinkage ( $\alpha_{DS}$ ), the prestressing losses and early age cracks reopening under constant pressurization loads.

- Service loads: during the operational phase, the air leakage rate through cracks is mainly dependent on their numbers (obtained during the early age phase), the prestressing losses in time but mostly the effective prestressing  $\sigma_{PREC}^T$  and pressurization  $\sigma_{PRES}^T$  loads applied on the structure in the principle tangential direction. It is worth noting that early age cracks' reopening is conditioned by a positive residual stress  $\sigma_{PRES}^T - \sigma_{PREC}^T$ .

- Transfer properties of concrete: the variability of concrete's intrinsic permeability  $k_0$  is shown to be one of the most influential inputs on the computed total air leakage rate compared to the rest of leakage inputs. The effect of roughness and shape parameter ( $\xi$  in eq. 7) is non-null and increases over time; however, it remains considerably less than the rest of THM-L inputs.

So, those inputs are the ones retained for uncertainty propagation in the next step

(metamodeling and reliability analysis).

From a computational point of view, and compared to a default OFAT-based LSA to the leakage model with  $2*N+1$  (N being the total number of inputs), the application of the HLSA allowed a cost reduction of 66%. This underlines the efficiency of the suggested method for the most influential inputs' selection and probabilistic model dimensional reduction.

### 4.3 Reliability analysis

For a given quantity of interest depending on N random and independent inputs, and for a selected maximal polynomial order q, the number of polynomial terms is of  $Q = \frac{(N+q)!}{N!q!} - 1$ .

1. The identification of the associated polynomial coefficients would then require  $(1+q)^N$  model calls (using the classical Gauss-Quadrature method). For the leakage response, considering N=9 inputs and limiting the polynomial order to  $q = 3$  [19], 220 terms need to be defined per RSV using 262144 model calls. Given the lognormal distribution of inputs in Tab. 1, the polynomial basis is of Hermite.

Eventually, the obtained metamodel of the total leakage rate through the VeRCoRs structure shows a Root-Mean-Square-Error around 1.8% which is judged satisfactory compared to the precision of the air leakage rate measurement on site.

Once obtained, the metamodel is used to:

- First, perform a GSA to verify and validate the HLSA [20]: Qualitatively, the importance of the same influential parameters is demonstrated through a more accurate GSA. However, in terms of contribution to the global variance, the GSA shows naturally more accurate results (Tab. 2). One should note that, given the inputs' distributions in Tab. 1, the variance of the total air leakage rate is due by about 45% to the early age cracks'

(represented by  $R_t, E, \alpha_{ES}, \alpha_{TH}$ ), by about 15% to the operational loads' (represented by  $\sigma_{PREC}, \sigma_{PRES}$ ), by about 30% to the hydric/hydraulic properties' (represented by  $C_{w,0}, B_w, k_0$ ).

**Table 2:** Sensitivity analysis of the THM-L behavior of the VeRCoRs structure considering the total air leakage rate as an output of interest

Outputs →	Evolution of the air leakage rate from instant A to instant B A= 1 operational year → B= 6 operational years Total dry air leakage rate	
	HLSA	GSA
	Input ↓	
$Q_{\infty}$	-	-
$C^P$	-	-
$B_w$	A: 41% B: 04%	A: 13% B: 01%
$C_{w,0}$	A: 41% B: 15%	A: 13% B: 01%
$E$	-	A: 09% B: 22%
$R_t$	-	A: 09% B: 22%
$\alpha_{ES}$	-	A: 04% B: 10%
$\alpha_{TH}$	-	A: 04% B: 10%
$\alpha_{DS}$	-	-
$\sigma_{PRES}^T$	A: 12% B: 64%	A: 23% B: 25%
$\sigma_{PREC}^T$	A: 00% B: 02%	-
$k_0$	A: 04% B: 03%	A: 24% B: 08%

- Second, achieve reliability analysis: Given the 1:3 reduced scale of the VeRCoRs mock-up, the air leakage rate thresholds of 1.5% and 1.1% are  $3^2=9$  times higher and are estimated at 10.1% and 13.5% respectively. Based on a deterministic model, the exceedance of such thresholds is expected after 5 operational years of the VeRCoRs mock-up (Fig. 5a).

Limited to such results, this means that repair and maintenance operations need to be expected at this operational time by filling cracks or covering the containment wall's surface with impermeable material to bring the leakage rate below the regulatory threshold. The area to be repaired depends on the amount of air leakage beyond 10.1%. Numerically, the amount to overcome is of 6.4% which can, for instance, be totally annihilated by closing

50% of early age cracks.

However, when accounting for the THM-L uncertainties, the risk of exceeding the regulatory threshold becomes non-null right after the second operational year and is around 40% towards the sixth (Fig. 5b). So operators need to expect repair and maintenance earlier than what the deterministic analysis predicts. The decrease of such non conformity risk is mainly dependent on the control of uncertainties of the model's inputs.

## 5 Conclusions

In this contribution, a global stochastic Thermo-Hydro-Mechanical modeling methodology with Leakage post-processing (THM-L) is suggested to simulate the ageing of large reinforced concrete structures under uncertainties. The method consist of (a) reducing the model's list of random inputs by performing a prior Hierarchized Local Sensitivity Analysis (HLSA) through the THM-L calculations and through time (b) defining a metamodel of THM-L response using Spectral-based Methods (c) applying Monte Carlo Methods (MCM) to the metamodel for probabilistic and reliability analysis.

The pertinence of such approach is demonstrated through the probabilistic analysis of the air leakage rate of nuclear containment buildings. Accordingly, the flowing conclusions are retained:

- The application of HLSA method led to the identification of 9 influential inputs from more than 60. Those parameters are representative of the dominant ageing phenomena: early age cracking ( $R_t, E, \alpha_{ES}, \alpha_{TH}$ ), operational loads ( $\sigma_{PREC}, \sigma_{PRES}$ ), hydric and drying properties ( $B_w, C_{w,0}$ ) and transfer properties ( $k_0$ ). The importance of the same phenomena is demonstrated using advanced GSA.

- Due to uncertainty propagation and amplification from one THM-L calculation step to the other and in time, the air

leakage results are strongly dependent on the inputs variation. It is, then, necessary to favor full THM-L stochastic approaches rather than deterministic ones for better risk assessment.

One can note that the developed strategy remains applicable for other case studies (full

scale NCBs, dams, reservoirs, etc.) and considering different quantities of interest for structural performance assessment (temperature, strain, stress, relative humidity, etc.).

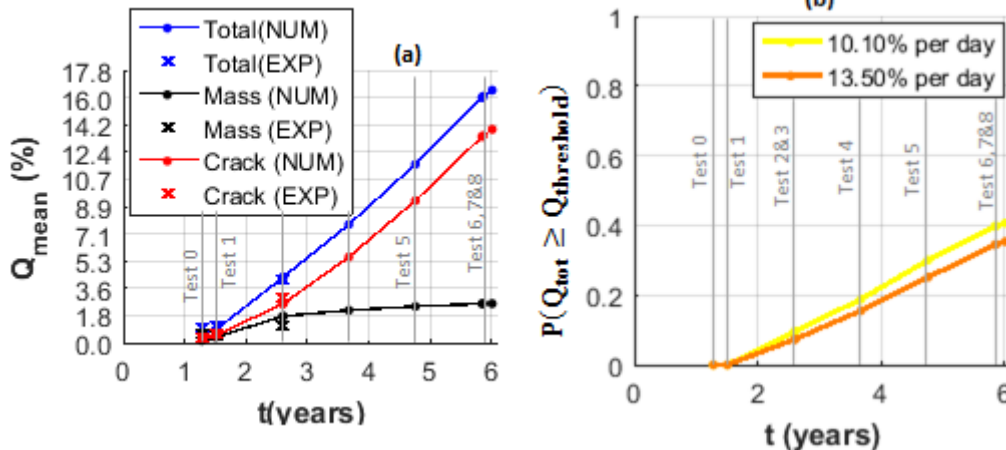


**Figure 5:** Evaluation of the total leakage rate through the VeRCoRs structure in time (a) deterministic predictive analysis (b) risk of exceeding the regulatory threshold

## 6 ACKNOWLEDGEMENT

This work was supported by EDF-SEPTEN/DTG/CIH within the Chair PERENITI agreement with the Grenoble INP Partnership Foundation and by the joint MACENA and ENDE project fund (ProjetIA-11-RSNR-0009 and ProjetIA-11-RSNR-0012).

## REFERENCES

- [1] Asali M., Capra B., Mazars J., Colliat J.B. (2016). Numerical Strategy for forecasting the leakage rate of inner containments in double-wall nuclear buildings. *Advanced concrete technology*. **14**: 408-420.
- [2] Chhun P., Buffo-Lacarrière L., Sellier A., 2016. Material and Geometric Heterogeneity Consideration for Cracking Risk Prediction of Young Age Behavior of Experimental Massive Reinforced Concrete Structure. *Key engineering materials*. **711**: 900-907.
- [3] Rossi P., Wu X., 1992. Probabilistic model for material behaviour analysis and appraisalment of concrete structures. *Magazine of Concrete Research*. **44**: 27-280.
- [4] de Larrard, T., Colliat J. B., Benboudjema F., Torrenti J. M., Nahas G., 2010. Effect of the young modulus variability on the mechanical behaviour of a nuclear containment vessel. *Nuclear engineering and Design*. **240**:4051–4060.
- [5] Vořechovský M., 2007. Interplay of size effects in concrete specimens under tension studied via computational stochastic fracture mechanics. *Solids and structures*. **44**:2715-2731.
- [6] Rastiello G., Tailhan J. L., Rossi P. Dal Pont S., 2015. Macroscopic probabilistic cracking approach for the numerical modeling of fluid leakage in concrete. *Solid and Structural Mechanics*. **7**: 1-16
- [7] Bouhjiti D. E.-M., Baroth J., Briffaut M., Dufour F., Masson B., 2018. Statistical modeling of cracking in large concrete structures under Thermo-Hydro-Mechanical loads: Application to Nuclear

- Containment Buildings. Part 1: Random field effects (Reference analysis). *Nuclear Engineering and design*. **333**:196-223.
- [8] Briffaut M., Benboudjema F., Torrenti J.-M., Nahas G., 2012. Effects of early age thermal behaviour on damage risks in massive concrete structures. *Civil and Environmental Engineering*. **16**: 589-605.
- [9] Granger L., Torrenti J.-M., Ithurrealde G., 1993. Delayed behavior of concrete in nuclear power plant containments: analysis and modeling. *4<sup>th</sup> Int. Rilem Symp. On creep and shrinkage of concrete. Barcelona. Spain*: 751-756.
- [10] Tailhan J.-L., Rossi P., Caucci A. M., 2014. Probabilistic modeling of cracking in concrete. *European Journal of Civil Engineering*. **18**: 770-779.
- [11] Dameron R.A., Rashid Y.R., Tang H.T., 1995. Leak area and leakage rate prediction for probabilistic risk assessment of concrete containments under severe core conditions. *Nuclear Engineering and Design*. **156**: 173-179.
- [12] Tang H.T., Dameron R.A., Rashid Y.R., 1995. Probabilistic evaluation of concrete containment capacity for beyond design basis internal pressures. *Nuclear Engineering and Design*. **157**: 455-467
- [13] Bouhjiti D. E.-M., Boucher M., Briffaut M., Dufour F., Baroth J., Masson B., 2018. Accounting for realistic Thermo-Hydro-Mechanical boundary whilst modeling the ageing of concrete in nuclear containment buildings: Model validation and sensitivity analysis. *Engineering Structures*. **166**: 314-338.
- [14] Bouhjiti D. E.-M., Baroth J., Dufour F., Masson B., 2018. Prediction of air permeability in large RC structures using a stochastic FE THM modeling strategy. Proceedings of the Conference on Computational modeling of concrete and concrete structures. *Euro-C. Bad Hofgastein, Austria*: 237-248.
- [15] Mazars, J., Hamon, F., Grange, S., 2015. A new 3D damage model for concrete under monotonic, cyclic and dynamic loadings. *Materials and structures*. **48**: 3779-3793
- [16] Bouhjiti D. E.-M., El Dandachy E. M., Dufour F., Dal Pont S., Briffaut M., Baroth J., Masson B., 2018. New continuous strain-based description of concrete's damage-permeability coupling. *Numerical and analytical methods in geomechanics*. 1-27.
- [17] Bouhjiti D. E.-M., 2018. Probabilistic analysis of cracking and tightness of reinforced and prestressed large concrete structures. *PhD thesis [in french]*. Univ. Grenoble Alpes, France.
- [18] Daniel C., 1973. One-at-a-time plans. *Amer. Statist. Assoc.* **68**: 353-360.
- [19] Baroth J., Breysse D., Schoefs F., 2011. Construction Reliability: Safety, Variability and Sustainability. Wiley-ISTE.
- [20] Sudret B., 2008. Global Sensitivity analysis using polynomial chaos expansions. *Reliab. Eng. Safety*. **93**:964-979